PACS numbers: 61.05.C −, 68.37.Lp

STUDY ON NANOPARTICLES OF ZnSe SYNTHESIZED BY CHEMICAL METHOD AND THEIR CHARACTERIZATION

M.P. Deshpande, S.H. Chaki, N.H. Patel, S.V. Bhatt, B.H. Soni

Department of Physics,
Sardar Patel University, 388120, Vallabh Vidyanagar, Gujarat, India
E-mail: vishwadeshpande@yahoo.co.in

The properties of semiconductor nanoparticles depend mainly on their shape and size due to high surface-to-volume ratio. The $II - VI$ semiconductors have many applications such as, LED, acousto-optical effects and biological sensors. The ZnSe nanoparticles have wide-ranging applications in laser, optical instruments etc. because it has wide band gap and transmittance range, high luminescence efficiency, low absorption coefficient. In recent years, much attention was paid on the preparation methods, performances and applications of ZnSe nanoparticles and thin solid films, and a lot of important accomplishments have been obtained. In the present study ZnSe nanoparticles were successfully prepared by reacting $Zn(CH_3COO)_2 \cdot 2H_2O$ and Na_2SeSO_3 at 343 K. The size of the crystallite was estimated by X-ray diffraction and TEM, whereas EDAX has confirmed of no foreign impurity inclusion in ZnSe nanoparticles. XRD shows the crystallite size of 5.68 nm and TEM gives a distribution ranging from 20 nm to 71 nm. A SEM image shows that the particles are spherical in a shape. Quantum confinement has resulted in the blue shift compared to bulk ZnSe as observed from the absorption spectra of particles dispersed in DMF. We obtained the photoluminescence spectra on these particles with two different excitation wavelength which shows broad band emission peak at 573 nm. Photoluminescence spectra taken with other excitation wavelength also gives sharp emission peaks at 484 nm, 530 nm, 551 nm and 600 nm.

Keywords: *ZnSe NANOPARTICLES, CHEMICAL METHOD.*

(Received 04 February 2011, in final form 18 March 2011)

1. INTRODUCTION

Several approaches and a lot of publications have been devoted to prepare and control the size and shape of $II - VI$ semiconductor nanoparticles. Among all semiconductor materials, the $II - VI$ semiconductor systems have many applications, such as light emitting diodes and acousto-optical effects and biological sensors [1-5]. Zinc selenide (ZnSe) is an important $II - VI$ semiconductor material, with a rather wide bulk direct bandgap energy (E_g = 2.7 eV) [6-7], and a small exciton Bohr diameter of 9 nm [12]. Zinc selenide is normally known to be an n-type semiconducting material [6-11].The synthesis of nanocrystalline ZnSe powders with tunable phase, morphology and size provides alternative variables in tailoring its physical and chemical properties [13-17]. The ZnSe nanoparticles have wide-ranging applications in laser, optical instruments, etc. because it has wide band gap (2.58 eV) and transmittance range (0.5 - 22 μm), high luminescence efficiency, low absorption coefficient, and excellent transparency to infrared

[18-20]. It is used to increase the open circuit voltage of solar cells [21]. It exhibits great potential for various optoelectronic and high-speed applications like blue-green light emitting diodes, photoluminescent and electroluminescent devices, lasers and thin film solar cells [22-23].

ZnSe nanocrystalline samples were mostly prepared by molecular beam epitaxy (MBE) [24], metalorganic chemical vapor deposition (MOCVD) [25] and organometallic vapor phase epitaxy (OMVPE) [26], Solvothermal or hydrothermal route [27-28], mechanochemical synthesis from Zn and Se granules [29]. Now days, a wide variety of methods have been employed for preparing zinc selenide (ZnSe) nanocrystals or nanoparticles with controlled size such as solvothermal [30], sol-gel method [31], and microemulsion technique [32]. An effective control over the particle size can be achieved by manipulating different parameters namely, concentration, molar ratio of the reactants, time of heating in chemical method [33, 34] and radiation doses in radiolytic method [35-36]. Recently, a variety of ZnSe nanostructured materials in various geometrical morphologies, including nanoparticles [37], rods [38], wires [39], belts [40], needles [41], saw and tube [42], plates [43], hollow microspheres constructed with nanoparticles [44], and flowerlike pattern of radially aligned nanoflakes [45], nanoribbons[46], nanowheels [47], nanorings [48], nanopowders [49] have successfully been prepared by various methods.

2. EXPERIMENTAL DETAIL

Chemicals used for the synthesis of ZnSe nanoparticles were zinc acetate [$Zn(CH_3COO)_2$], sodium selenosulphate (Na_2SeSO_3), ammonia solution (25 %) [NH_3], hydrazine hydrate (80 %) [$N_2H_4.H_2O$], sodium hydroxide [NaOH], selenium powder (99 % purity) [Se], sodium sulfite [Na_2SO_3]. All chemicals used were A.R. grade. Here zinc acetate work as Zn^{2+} ion source, Na_2SeSO_3 as Se^{2-} ion source, ammonia as a complexing agent, hydrazine hydrate as catalyst and sodium hydroxide as a pH adjustor.

The 0.25 M sodium selenosulphate solution was prepared by mixing 2.36 gm selenium powder (99% purity) with 9.48 gm anhydrous sodium sulfite in 120 ml of distilled water with constant stirring for 8 h. It was sealed and kept overnight, since on cooling, a little selenium separated out from the solution. It was then filtered to obtain a clear solution. A 25 ml of (0.5 M) zinc acetate solution was taken in a beaker of 200 ml capacity. To, it 1ml of hydrazine hydrate (80 %) was added under a constant stirring. To this, under constant stirring, a sufficient amount of ammonium solution (25 %) was added to dissolve the turbidity of resultant solution. The desired pH of the resultant solution was adjusted by adding sodium hydroxide (1 M) solution. Then the reactant vessel was kept at 343 K in a constant temperature water bath. When appropriate temperature of 333 K was reached, sodium selenosulphate (0.25 M, 25 ml) solution was added to the bath. Then heated continuously at constant 343 K temperature for 3 - 4 hour and cooled to the room temperature. White colored precipitates obtained at the bottom of the beaker were filtered, washed a number of times in distilled water and dried in a vacuum.

3. RESULT AND DISCUSSION

3.1 Chemical mechanism

Sodium selenosulphate hydrolysis in the solution to give Se^{2-} ions according to,

$$Na_2SeSO_3 + OH^- \rightarrow Na_2SO_4 + HSe \qquad (1)$$

$$HSe^- + OH^- \rightarrow H_2O + Se^{2-}. \qquad (2)$$
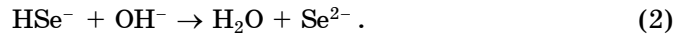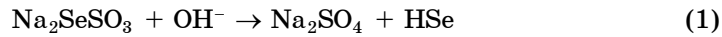
When hydrazine hydrate is added in Zinc Acetate it forms the ions of Zn^{+2}

$$mZn(CH_3COO)_2 + nN_2H_4 \rightarrow [Zn(CH_3COO)_2]_m \cdot [N_2H_4]_n \qquad (3)$$

$$[Zn(CH_3COO)_2]_m \cdot [N_2H_4]_n \rightarrow mZn^{2+} + nN_2H_4 + 2m(CH_3COO)^{2-}. \qquad (4)$$
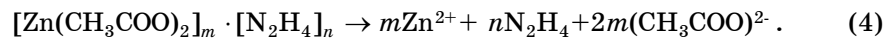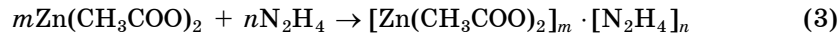
When ammonia solution is added to this Zn-salt solution it gives the complex of zinc tetra-amine ion $[Zn\,(NH_3)_4^{2+}]$ as,

$$Zn^{2+} + 4NH_3 \rightarrow Zn\,(NH_3)_4^{2+}. \qquad (5)$$
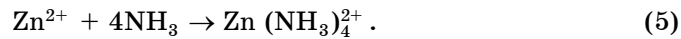
Then $Zn\,(NH_3)_4^{2+}$ react with Se^{2-} ions that result in the formation of ZnSe nanoparticles as follows:

$$Zn \cdot (NH_3)_4^{2+} + Se^{2-} \rightarrow ZnSe + 4NH_3. \qquad (6)$$
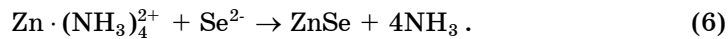
3.2 Energy dispersive analysis of X-ray (EDAX)

The compositions of synthesized ZnSe nanoparticles were determined by the spectra obtained by Energy dispersive analysis of X-rays (EDAX) which is shown in Fig. 1. This analysis was carried out using Philips EM 400 electron microscope. It is reflected from the EDAX spectra that no foreign impurities are present in the sample.
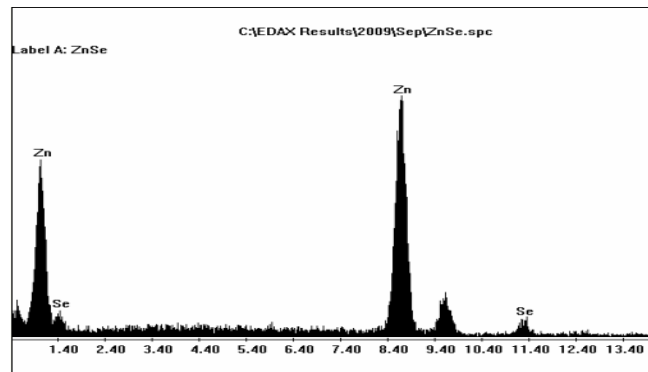
Fig. 1 − EDAX Spectra of ZnSe nanoparticles

3.3 X-ray diffraction (XRD)

The X-ray diffractogram of ZnSe nanocrystallites synthesized by chemical method is shown in Fig. 2 and indexed based on hexagonal system. This analysis was carried out using XRD diffractometer (powder) Philips Xpert MPD. The values of the lattice parameter determined from the X-ray diffractogram using powder X software which clearly matches with the reported values of lattice parameter of

ZnSe (JCPDS No. 15-0105). The presence of a relatively sharp peak on a background of a wider peak suggest that both large and small grains are collected together. The peaks (N) are not identified as ZnSe and may be due to zinc complex formed during the reaction [50].
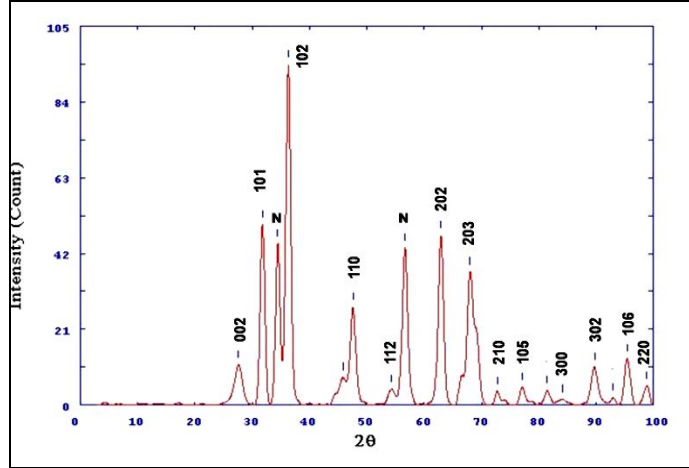
Fig. 2 − X-ray diffractogram of ZnSe nanocrystallites

We used Scherrer's formula [51-53] for calculating the crystallite size which is given by,

$$t = k\lambda/\beta_{2\theta}\cos\theta$$

where, t is the crystallite size, k is the Scherrer constant whose value is chosen to be unity by assuming the particle to be spherical, λ is the wavelength of X-ray beam, θ is the Bragg angle. $\beta_{2\theta}$ is the width at half the maximum intensity measured in radians.

$$\beta_{2\theta} = \sqrt{(FWHM_{obs})^2 - (FWHM_r)^2}$$

$FWHM_{obs}$ is observed reflection from ZnSe nanocrystallite. $FWHM_r$ is instrumental function of the diffractometer [54].

This technique gives us the rough estimate of crystallite size ranging from 5 nm to 9 nm due to correction factor involved in the Scherrer's equation. Fig. 3 shows Hall-Williamson plots for ZnSe nanocrystallites. The most widespread method used for estimating the nanocrystallite sizes is the calculation of line broadening by the Williamson-Hall method [55], which not only uses the Scherrer's formula [51-53] but also takes into account the microstrain of nanocrystals. This plot requires large number of nonoverlapping reflections. For this reason, we used the Williamson-Hall method to calculate the size of particles and also to obtain information of the strain from the full width at half maximum (FWHMs) of the diffraction peaks. The FWHMs (β) can be expressed as a linear combination of the contributions from the strain (ε) and crystallite size (L) through the following relation [56].

$$\frac{\beta\cos\theta}{\lambda} = \frac{K}{L} + \frac{4\varepsilon\sin\theta}{\lambda}$$

The plot of $\beta\cdot\cos\theta/\lambda$ versus $(\sin\theta/\lambda)$ for ZnSe nanocrystallites which is straight line. The slope of the plot gives the amount of residual strain, which turns out to be $-$ 0.0026 for ZnSe nanocrystallite. The reciprocal of intercept on the $(\beta\cdot\cos\theta/\lambda)$ axis gives the average crystallite size as ~ 5.68 nm. The negative value of residual strain indicates the presence of compressive strain in ZnSe nanocrystallites.
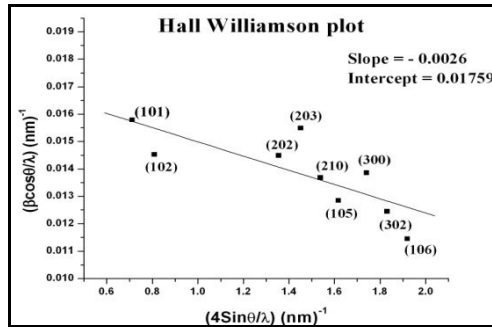
Fig. 3 − *Hall-Williamson plot for ZnSe nanocrystallite*

3.4 Transmission electron microscopy (TEM)

The TEM image of ZnSe nanoparticles is shown in Fig. 4. This analysis was carried out using Philips, Tecnai 20 microscope. The TEM morphology shows particles have spherical shape. Nanoparticle sizes determined from Fig. 4a ranges between 20 - 31 nm and Fig. 4b ranges between 17 - 71 nm which are showing higher values than those obtained from Scherrer's equation used in X-ray diffractogram. This indicates that the size distribution of nanocrystallites is not uniform and varies from 17 nm to 71 nm.

a   b
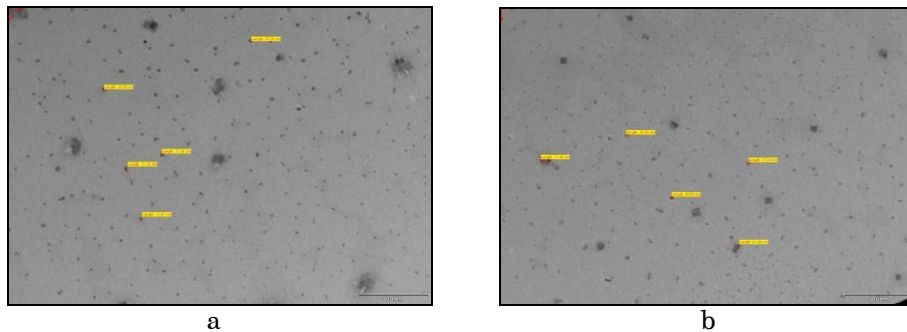
Fig. 4 − *Shows images of ZnSe nanoparticles (a) and (b)*

Fig. 5 shows diffraction pattern which is indicating that ZnSe nanocrystallites are polycrystalline in nature. This diffraction pattern shows (112), (102), (202), (210) reflections which are corresponding to the hexagonal phase of ZnSe nanocrystallites and there by matching with the X-ray diffraction pattern.
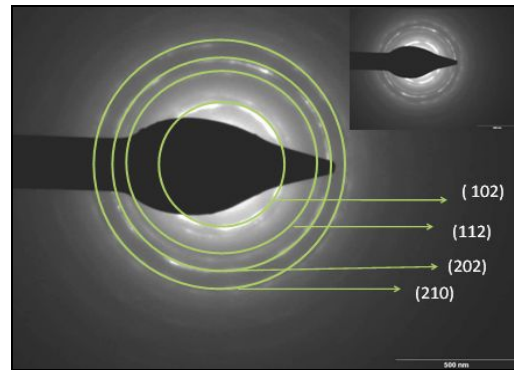
Fig. 5 − Selected area diffraction pattern for ZnSe nanocystallites
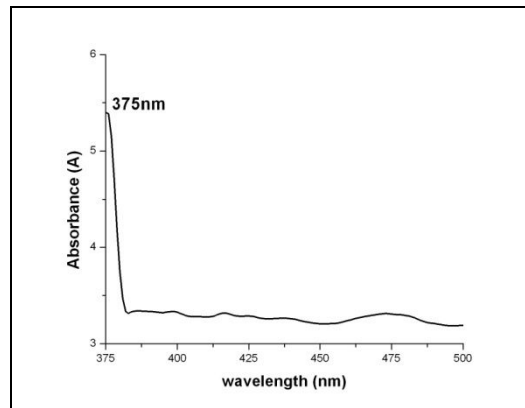
Fig. 6 − Absorption spectra for ZnSe nanoparticles

3.5 Absorption spectra of ZnSe nanoparticles

Absorption spectroscopy is a good way to study any change in the particle size which could occur during the aggregation of the particles. The ZnSe nanoparticles synthesized were dispersed in DiMethylFormamide **(DMF)** to obtain the absorption spectra in the UV-VIS region. This analysis was carried out using Perkin-Elmer Lambda **19** spectrophotometer. Fig. **6** shows the absorption spectra for ZnSe nanoparticles and it can be seen that the absorption edge lies at **375** nm with the band gap at **3.3** eV. Comparing with that of bulk material **(460 nm, 2.7 eV)**, it is believed that the blue shift in the absorption peak was caused by the quantum confinement effect.

The size of the prepared particles can be calculated from the spectral data using Wang equation **[53]** given as,

$$\Delta E = \left(\frac{\hbar^2 \pi^2}{2R^2} \right) \left(\frac{1}{m_e} + \frac{1}{m_h} \right) - \frac{1.8 e^2}{pR}$$

which reduces as,

$$E = \sqrt{E_g^2 + 2E_g h^2 \left(\frac{\pi^2}{R^2 m^*} \right)} \, ,$$

where, E_g is the bulk band gap, E is the energy gap of the size quantized ZnSe, 'R' is the radius of the particle and m^* is the effective mass with $m_e = 0.21 \, m_o$ and $m_h = 0.06 \, m_0$ for ZnSe [61]. By substituting our values of $E_g = 2.7$ eV for bulk ZnSe [59, 60] and $E = 3.3$ eV for ZnSe nanoparticles obtained from absorption spectra, we get the diameter of particles as 11.97 nm which shows close agreement with the values obtained from the XRD data but not with TEM.

3.6 Scanning electron microscope

The Scanning electron microscopy (SEM) image of the ZnSe nanoparticles is shown in Fig. 7a and Fig. 7b. These figures show that the product particles are spherical in shape and agglomeration is also observed. This agglo-meration is caused because we did not use any capping agent for synthesis of ZnSe nanoparticles.

a   b
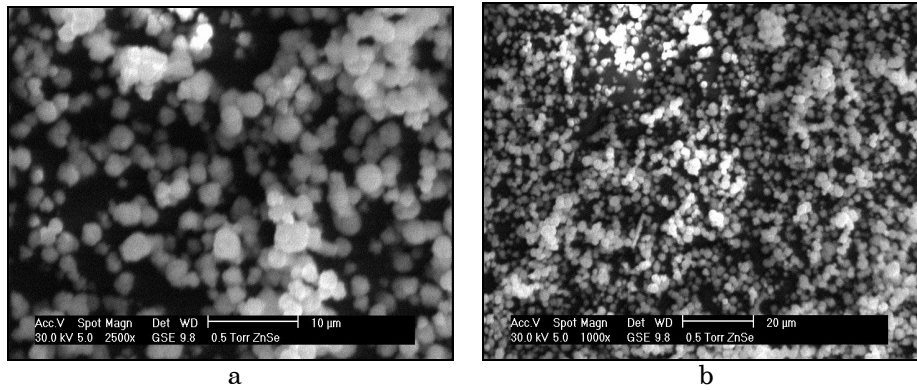
Fig. 7 − SEM micrograph of ZnSe nanoparticles

3.7 Photoluminescence of ZnSe nanoparticles

Photoluminescence spectra for ZnSe nanoparticles is shown in Fig. 8a. This analysis was carried out using FluoroMax − 4 Spectrofluorometer. It shows broad band emission between 500 to 650 nm which is due to deep level emission [62]. Photoluminescence spectra of ZnSe nanoparticles taken by us with two different excitation wavelength ($\lambda_e = 371, \, 407$ nm) is shown in Fig. 8a. It shows broad band emission peak at 573 nm with a red shift about 94 and 58 nm compared to bulk ZnSe at 465 nm respectively [63-65].This emission at 573 nm exhibits a Stokes shift.

We also took photoluminescence spectra of ZnSe nanoparticles with other excitation wavelength also ($\lambda_e = 434$ nm, 439 nm, 484 nm, 503 nm) as shown in Fig. 8b. Here we get sharp emission peak at 484 nm, 530 nm, 551 nm, 600 nm when it excited at 434 nm, 439 nm, 484 nm, 503 nm respectively and red shift of about 19 nm, 65 nm, 86 nm, 135 nm is observed compared to bulk ZnSe at 465 nm [63-65].
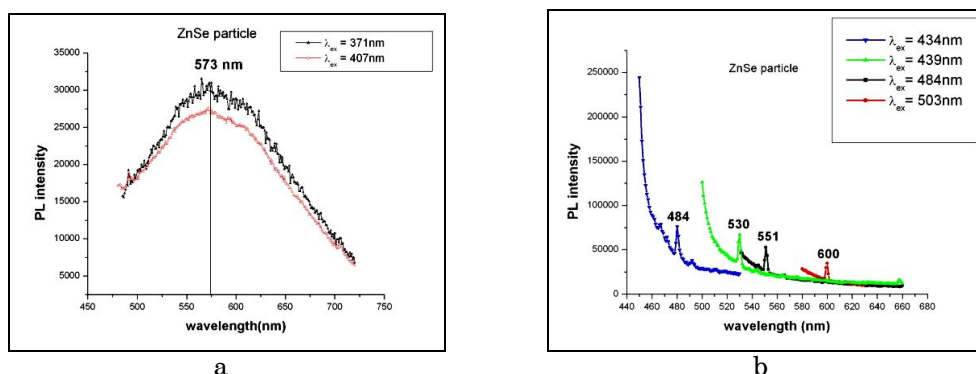
Fig. 8 − (a) and (b) shows PL spectra of ZnSe nanoparticles

4. CONCULSION

EDAX analysis confirms that the synthesized nanoparticles of ZnSe and do not contain any foreign element in them. Powder X-ray diffractogram shows that ZnSe nanocrystallites are polycrystalline in nature and belong to the hexagonal phase. The crystallite size calculated by using Scherrer's formula comes out to be between 5 - 9 nm and the lattice parameter is about $a = 3.98$ Å and $c = 6.55$ Å° which matches nearly with JCPDF files. From the Hall-Williamson plot the value of strain comes out to be $− 0.0026$ and average crystallite size is 5.68 nm. The TEM image shows that the particle size ranges between 17 - 71 nm and selected area diffraction pattern indicated that the synthesized ZnSe nanocrystallites are polycrystalline in nature. The absorption spectra show blue shift in the absorption edge at 375 nm for ZnSe nanoparticles in comparison to bulk ZnSe which is observed at 460 nm. The SEM image shows that the ZnSe nanoparticles are spherical in shape with agglomeration The Photoluminescence spectra shows red shift at 573 nm for ZnSe nanoparticles in comparison to bulk ZnSe which is observed at 465 nm. Another Photoluminescence spectra show red shift at 484 nm, 530 nm, 551 nm, 600 nm for ZnSe nanoparticles in comparison to bulk ZnSe which is observed at 465 nm.

ACKNOWLEGMENT

REFERENCES

1. V.L. Colvin, M.C. Schlamp, A.P. Alivisatos, *Nature* **370,** 354 (1994).
2. W.C.W. Chan, S. Nie, *Science* **281,** 2016 (1998).
3. I.V. Kityk, J. Kasperczyk, B. Sahraoui, M.F. Yasinskii, *Polymers* **38,** 4803 (1997).
4. G.P. Mitchell, C.A. Mrkin, R.L. Letsinger, *J. Am. Chem. Soc.* **121,** 8122 (1999).
5. I.V. Kityk, Phys. Solid State **33,** 1026 (1991).
6. M.A. Russak, *J. Electrochem. Soc.* **129,** 542 (1982).

7. O.V. Krylov, *Catalysis by Nonmetals* (Academic Press: New York: 1970).
8. J. Gautron, P. Lemmason, C. Rabuyo, R. Tribaulet, *J. Electrochem. Soc.* **126, 1868** (1979).
9. P. Lemasson and J. Gautron, *J. Electroanal. Chem.* **119, 289** (1989).
10. P. Lemasson, *J. Cryst. Growth* **72, 405** (1985).
11. G. Hodes, D. Cahen, J. Manassen, M. David, *J. Electrochem. Soc.* **127, 544** (1980).
12. N. Kumbhojkar, S. Mahamuni, V. Leppert. S.H. Risbud, *Nanostruct. Mater.* **10 No2, 117** (1998).
13. A.B. Panda, S. Acharya, S. Efrima, Y. Golan, *Langmuir* **23, 765** (2007).
14. H. Gong, H. Huang, L. Ding, M.Q. Wang, K.P. Liu, *J. Cryst. Growth* **288, 96** (2006).
15. Y. Jiao, D.B. Yu, Z.R. Wang, K. Tang, X.Q. Sun, *Mater. Lett.* **61, 1541** (2007).
16. H.N. Wang, F.L. Du, *Cryst. Res. Technol.* **41, 323** (2006).
17. Q. Peng, Y.J. Dong, Y.D. Li, *Angew. Chem. Int. Ed.* **115, 3135** (2003).
18. A.P. Alivisatos, *Science* **271, 933** (1996).
19. H. Luo, J.K. Furdyna, *Semicond. Sci. Technol.* **10, 1041** (1995).
20. Q. Peng, Y.J. Dong, Y.D. Li, *Angew. Chem. Int. Ed.* **42, 3027** (2003).
21. T.L. Chu, S.S. Chu. *Prog. Photovoltaics Res. Appl.* **1,** 31 (1993).
22. S.T. Lakshmikumar, A.C. Rastogi, *Thin Solid Films* **259,** 150 (1995).
23. C.D. Lokhande, P.S. Patil, H. Tributsch, A. Ennaoni, *Sol. Energ. Mat. Sol. C.* **55, 379** (1998).
24. B.P. Zhang, T. Yasuda, Y. Segawa, H. Yaguchi, K. Onabe, E. Edamatsu, T. Itoh, *Appl. Phys. Lett.* **70, 2413** (1997).
25. C.E.D. Bourret, *Appl. Phys. Lett.* **68, 2418** (1996).
26. M.C. Klein, F. Hache, D. Ricard, C. Flytzanis, *Phys. Rev. B* **42, 11123** (1990).
27. Y.D. Li, Y. Ding, Y.T. Qian, Y. Zhang, L. Yang, *Inorg. Chem.* **37, 2844** (1998).
28. Z.X. Deng, C. Wang, X.M. Sun, Y.D. Li, *Inorg. Chem.* **41** 869 (2002).
29. M. Abdel Rafea, *J. Sci.-Mater. El.* **18, 415** (2007).
30. H. Gong, H. Huang, L. Ding, M. Wang, K. Liu, *J. Cryst. Growth* **288, 96** (2006).
31. L.S. Li, N. Pradhan, Y. Wang, X. Peng, *Nano Lett.* **4, 2261** (2004).
32. G.N. Karanikolos, P. Alexandridis, G. Itskos, A. Petrou, T.J. Mountziaris, *Langmuir* **20, 550** (2004).
33. D.Crouch, S. Norager, P. O'Brien, J.H. Park, N. Pickett, *Phil. Trans. R. Soc. Lond. A* **361, 297** (2003).
34. A. Priyam, A. Chatterjee, S.C. Bhattacharyya, A. Saha, *J. Cryst. Growth* **304, 416** (2007).
35. A. Datta, A. Priyam, S. Chatterjee, A.K. Sinha, S.N. Bhattacharya, A. Saha, *Colloids Surf. A* **301, 239** (2007).
36. A.H. Souici, N. Keghouche, J.A. Delaire, H. Remita, M. Mostafavi, *Chem. Phys. Lett.* **422,** 25 (2006).
37. W.Z. Wang, Y. Geng, P. Yan, F.Y. Liu, Y. Xie, Y.T. Qian, *J. Am. Chem. Soc.* **121, 4062** (1999).
38. J. Yang, C. Xue, S.H. Yu, J.H. Zeng, Y.T. Qian, *Angew. Chem.* **41, 4697** (2002).
39. X.T. Zhang, Z. Liu, Y.P. Leung, Q. Li, S.K. Hark, *Appl. Phys. Lett.* **83, 5533** (2003).
40. T.Y. Zhai, H.Z. Zhong, Z.J. Gu, A.D. Peng, H.B. Fu, Y. Ma, Y.F. Li, J.N. Yao, *J. Phys. Chem. C* **111, 2980** (2007) .
41. H.Z. Fu, H.Y. Li,W.Q. Jie, L. Yang, *J. Cryst. Growth* **289, 440** (2006).
42. A. Colli, S. Hofmann, A.C. Ferrari, C. Ducati, F. Martelli, S. Rubini, A. Franciosi, J. Robertson, *Appl. Phys. Lett.* **86, 153103** (2005).
43. Z.X. Deng, C. Wang, X.M. Sun, Y.D. Li, *Inorg. Chem.* **41, 869** (2002).
44. Q. Peng, Y.J. Dong, Y.D. Li, *Angew. Chem. Int. Ed.* **42, 3027** (2003).
45. J. Du, L.Q. Xu, G.F. Zou, L.L. Chai, Y.T. Qian, *Mater. Chem. Phys.* **103, 441** (2007).
46. Y. Jiang, X.M. Meng, W.C. Yiu, J. Liu, J.X. Ding, C.S. Lee, S.T. Lee, *J. Phys. Chem. B* **108, 2784** (2004).

47. L. Jin, W.C.H. Choy, Y.P. Leung, T.I. Yuk, H.C. Ong, J.B. Wang, *J. Appl. Phys.* **102,** 044302 (2007).
48. Y.P. Leung, W.C.H. Choy, I. Markov, G.K.H. Pang, H.C. Ong, T.I. Yuk, *Appl. Phys. Lett.* **88,** 183110 (2006).
49. S.V. Pol, V.G. Pol, J.M. Calderon-Moreno, S. Cheylan, A. Gedanken, *Langmuir* **24,** 10462 (2008).
50. M.S. Selim, R. Seoudi, A.A. Shabaka, *Materials Letters* **59,** 2650 (2005).
51. H.P. Klug, L.E. Alexander, J. Wiley & Sons X-Ray Spectrometry, **4,** A18 (1974).
52. J. Du, L. Fu, Z. Liu, B. Han, Z. Li, Y. Liu, Z. Sun, D. Zhu, *J. Phys. Chem. B* **109,** 12772 (2005).
53. H.J. Watzke, J.H. Fendler, *J. Phys. Chem.* **91,** 854 (1987).
54. N.S. Belova, A.A. Rempel, *Inorganic Materials, 40, 3* (2004).
55. B. Andersson, J. Gjonnes, A.R. Forouhi, *J. less-Common Met.* **61,** 273 (1978).
56. W. Wei-Yu, J.N. Schulman, T.Y. Hsu, F. Uzi, *Appl. Phys. Lett.* **51,** 710 (1987).
57. B. Nelson, D.P. Riley, *Proc. Phys. Soc.* **57,** 160 (1945).
58. L.V. Azaroff, M. Buerger, *The Powder Method in X-ray Crystallography* (New York: McGraw-Hill: 1958).
59. M.A. Russak, J. Reichman *J. Electrochem Soc.* **129,** 542 (1982).
60. O.V. Krylov, Catalysis by Nonmetals (Academic Press, New York), 258 (1970).
61. D.W. Palmer, *Properties of the II − VI compound semiconductors* www.semiconductors.co.uk (2008).
62. N. Hizem, A. Kalboussi, R. Adhiri, A. Souifi, *J. Microelectron.* **38,** 496 (2007).
63. M.A. Hines, P. Guyot-Sionnest, *J. Phys. Chem, B* **102,** 3655 (1998).
64. F.T. Quinlan, J. Kuther, P. Stroeve, *Langmuir* **16,** 4049 (2000).
65. S. Bhaskar. P.S. Dobal, B.K. Katryar, *J. Appl. Phys.* **85,** 439 (1999).